Sensors and Materials, Vol. 35, No. 3 (2023) 1059–1068
MYU Tokyo

S & M 3228

Enhancement of Microwave Dielectric Properties by Ti^{4+} Substitution at B-site of Mg_2SnO_4 Ceramics for Temperature Sensor

Yih-Chien Chen,* Chun-Hao Tai, and Rei-Shin Chen

Department of Electrical Engineering, Lunghwa University of Science and Technology,
No. 300, Sec.1, Wanshou Rd., Guishan District, Taoyuan City 333326, Taiwan

(Received February 26, 2022; accepted December 12, 2022)

Keywords: ceramics, electronic characterization, dielectric properties, temperature sensor

The microwave dielectric properties of $Mg_2(Sn_{1-x}Ti_x)O_4$ ceramics were examined with a view to their exploitation as a temperature sensor. $Mg_2(Sn_{1-x}Ti_x)O_4$ ceramics were prepared by the conventional solid-state method with various sintering temperatures. X-ray diffraction patterns of the $Mg_2(Sn_{0.97}Ti_{0.03})O_4$ ceramic revealed no significant variation of the phase with the sintering temperature. An apparent density of 4.54 g/cm^3, a dielectric constant (ε_r) of 8.3, quality factor ($Q \times f$) of 75000 GHz, and a temperature coefficient of resonant frequency (τ_f) of −57 ppm/°C were obtained for the $Mg_2(Sn_{0.97}Ti_{0.03})O_4$ ceramic that was sintered at 1550 °C for 4 h. The development procedure and test results for a dielectric resonator antenna temperature sensor are also reported. The resonating frequency measured at 25 °C was 17.32 GHz and a sensitivity of −0.97 MHz/°C was successfully achieved.

1. Introduction

In recent years, the smart grid has attracted much attention. The intelligentization of high-voltage switchboards has become a core feature of smart grids, and temperature sensors play a very important role in this intelligentization. At present, there are a variety of commercial wired temperature sensors, such as those based on the sound radiation method, transient-to-ground voltage method, ultrahigh-frequency method, IR temperature measurement method, optical fiber temperature method, thermal image detection method, and wireless temperature detection method. Wired sensors require cables and connectors, which are prone to failure at high temperatures. To be suitable for high-temperature environments, wireless transmission methods are required to transmit the obtained sensing data to the remote monitoring host server.

Wireless temperature sensors are an important component in the development of smart grids and are widely used in environmental monitoring. Wireless temperature sensors are divided into electronic chip wireless temperature sensors and chipless wireless temperature sensors. Electronic chip wireless temperature sensors include integrated circuit components such as a microcontroller, signal transmission, and power supply. Their advantages include a long-distance

*Corresponding author: e-mail: ee049@mail.lhu.edu.tw
https://doi.org/10.18494/SAM4040

ISSN 0914-4935

reading range, high compatibility, and low detection limit. Data can be collected and processed by a wireless sensing network. However, owing to the characteristics of semiconductor materials, electronic chip wireless temperature sensors cannot be applied in a high-temperature environment. Because chipless temperature sensors do not require integrated circuit components such as signal transmission and a power supply, they can operate at high temperatures. Moreover, the ambient temperature can be simultaneously monitored through reflection[1] using the phase, amplitude, or frequency modulation of the reflected signal.[2–4]

*M*O–SnO_2 (*M* = Ca, Sr, and Ba) ceramics are known for their low dielectric constant and small loss tangent.[3,4] Mg_2SnO_4 ceramics exhibit a dielectric constant of 8.41, a quality factor ($Q \times f$) of 55100 GHz, and a temperature coefficient of resonant frequency (τ_f) of −62.0 ppm/°C when sintered at 1550 °C for 4 h.[5] Since the radius of Ti^{4+} ions (0.0605 nm) is similar to that of Sn^{4+} ions (0.069 nm), Sn^{4+} ion can be replaced with a Ti^{4+} ion to form $Mg_2(Sn_{1-x}Ti_x)O_4$. In this investigation, $Mg_2(Sn_{1-x}Ti_x)O_4$ ceramics were synthesized and some of the Sn^{4+} ions were substituted with Ti^{4+} ions to improve their microwave dielectric properties. Moreover, the effect of sintering temperature on the microwave dielectric properties of $Mg_2(Sn_{1-x}Ti_x)O_4$ ceramics was studied. $Mg_2(Sn_{1-x}Ti_x)O_4$ ceramics was synthesized by the conventional mixed-oxide method and were demonstrated to have superior microwave dielectric properties to Mg_2SnO_4 ceramics. The microwave dielectric properties of $Mg_2(Sn_{1-x}Ti_x)O_4$ ceramics were found to vary with the degree of Ti^{4+} substitution and the sintering temperature. Various microwave dielectric properties were analyzed by densification, X-ray diffraction (XRD), and observation of their microstructures. In addition, a $(Mg_{0.93}Ni_{0.07})2SnO_4$-based dielectric resonant antenna (DRA) temperature sensor was fabricated. Its applicability to temperature sensing was examined, including its sensitivity and linearity. The results of this study demonstrate the feasibility of applying $Mg_2(Sn_{1-x}Ti_x)O_4$ ceramics in dielectric resonator temperature sensors used at ultrahigh temperatures as well as in harsh environments.

2. Materials and Methods

The starting raw chemicals were highly pure $4MgCO_3 \cdot Mg(OH)_2 \cdot 4H_2O$ (43.5%), SnO_2 (99.9%), and TiO_2 (99.9%) powders. The prepared compounds had the formula $Mg_2(Sn_{1-x}Ti_x)O_4$ (x = 0.01, 0.03, 0.05). Specimens were prepared by the conventional mixed-oxide method. The raw materials were weighed out in stoichiometric proportions, ball-milled in alcohol, dried, and then calcined at 1200 °C for 4 h. The calcined powder was re-milled for 12 h using polyvinyl alcohol (PVA) solution as a binder. The obtained powder was then crushed into a fine powder through a sieve with a 200 mesh. The obtained fine powder was then axially pressed at 2000 kg/cm^2 into pellets with a diameter of 11 mm and a thickness of 6 mm. The specimens thus obtained were then sintered at temperatures of 1450–1600 °C for 4 h in air. The heating and cooling rates were both set to 10 °C/min. Following sintering, the phases of the samples were investigated by XRD. An X-ray Rigaku D/MAX-2200 spectrometer was used with CuKα radiation (at 30 kV and 20 mA) and a graphite monochromator in the 2θ range of 20–80°. Scanning electron microscopy (SEM; JEOL JSM-6500F) was utilized to elucidate the microstructures of the specimens. The apparent densities of the specimens were measured by the Archimedes method using distilled water.

The microwave dielectric properties of the specimens were measured using the post resonator method developed by Hakki and Coleman,[6] for which we utilized cylindrical specimens of diameter D and length L. The specimens used for microwave dielectric property measurements had an aspect ratio D/L of approximately 1.6, which is in the range identified as acceptable by Kobayashi and Katoh.[7] The cylindrical resonator was sandwiched between two conducting plates. Two small antennas were positioned in the vicinity of the specimen to couple the microwave signal power into or out of the resonator. The other ends of the antennas were connected to a Keysight N5222A network analyzer. The resonance characteristics depended on the size and microwave dielectric properties of the specimen. The microwave energy was coupled with the specimen using electric-field probes. The TE_{011} resonant mode was optimal for determining the dielectric constant and loss factor of the specimen. The Keysight N5222A network analyzer was used to identify the TE_{011} resonant frequency of the dielectric resonator, and the dielectric constant and quality factor were calculated. The measurement scheme was the same as that for measuring the dielectric constant. The test cavity was placed in a chamber and the temperature was increased from 25 to 75 °C. The τ_f value (ppm/°C) was determined by noting the change in resonant frequency, where f_1 and f_2 represent the resonant frequencies at T_1 and T_2, respectively.

$$\tau_f = \frac{f_2 - f_1}{f_1(T_2 - T_1)} \tag{1}$$

3. Results and Discussion

Figure 1 displays the XRD patterns of $Mg_2(Sn_{0.97}Ti_{0.03})O_4$ ceramics sintered at 1450–1600 °C for 4 h. $Mg_2(Sn_{0.97}Ti_{0.03})O_4$ (ICDD-PDF #73-1625) is the main crystalline phase, which is

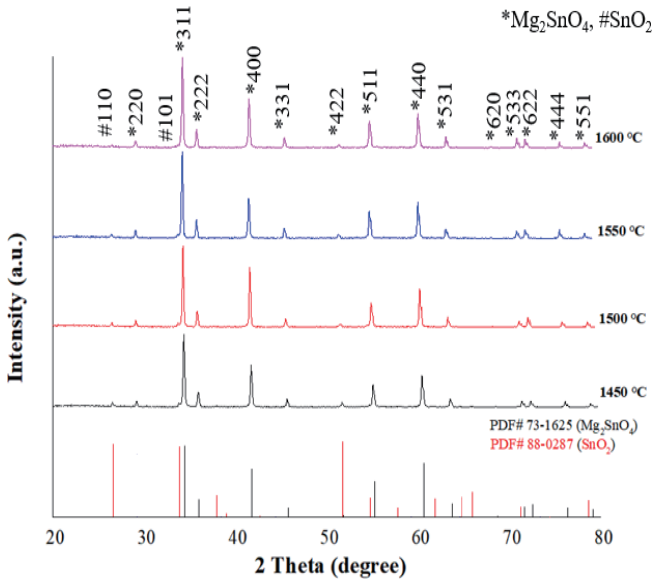

Fig. 1. (Color online) XRD patterns of $Mg_2(Sn_{0.97}Ti_{0.03})O_4$ ceramics sintered at 1450–1600 °C for 4 h.

accompanied by small amounts of MgO and SnO_2 as secondary phases, indicating that some of the $MgSnO_3$ might have formed in the initial stages. The parallel reactions are expressed as reactions (2) and (3); $MgSnO_3$ is unstable at high temperatures and thermally decomposes into Mg_2SnO_4 and SnO_2 [reaction (4)].

$$MgO + SnO_2 \rightarrow MgSnO_3 \tag{2}$$

$$2MgO + SnO_2 \rightarrow Mg_2SnO_4 \tag{3}$$

$$MgSnO_3 \rightarrow 0.5Mg_2SnO_4 + 0.5SnO_2 \tag{4}$$

These results are consistent with those of Pfaff.[8] The SnO_2 intensity decreased at high sintering temperatures, revealing the evaporation of SnO_2 at high temperatures according to the reaction[9]

$$SnO_2(s) \rightarrow SnO\ (g) + 0.5O_2(g). \tag{5}$$

The relative integrated intensity demonstrated the difference in the amount of SnO_2 more clearly than the XRD patterns.[10] The relative integrated density can be assumed to be represent the amount of a phase present. The relative integrated intensity of SnO_2 was evaluated from the most intense lines of each phase as follows.

$$\text{Relative intensity of } SnO_2 = \frac{I_{SnO_2(110)}}{I_{Mg_2(Sn_{0.97}Ti_{0.03})_4(311)} + I_{SnO_2(110)}} \times 100 \tag{6}$$

The amount of SnO_2 decreased from 5.6 to 2.1% as the sintering temperature increased from 1450 to 1600 ℃, in agreement with reaction (5). The formation of secondary phases of SnO_2 and MgO affected the microwave dielectric properties of $Mg_2(Sn_{0.97}Ti_{0.03})O_4$ ceramics.

Figure 2 shows the microstructures of $Mg_2(Sn_{0.97}Ti_{0.03})O_4$ ceramics following sintering for 4 h at different temperatures. The specimens were not dense, and grains did not grow after sintering at 1450 ℃ for 4 h, potentially degrading the microwave dielectric properties of the specimens. A comparison of the microstructures of the specimens sintered at different temperatures indicated that the average grain size increased from 16.09 to 43.49 μm as the sintering temperature increased from 1500 to 1600 ℃. The pores almost disappeared upon sintering at 1550 ℃ for 4 h.

Figure 3 shows the apparent densities of the $Mg_2(Sn_{1-x}Ti_x)O_4$ ceramics with different degrees of Ti^{4+} substitution following sintering at 1450–1600 ℃ for 4 h. The theoretical density of Mg_2SnO_4 ceramics is 4.77 g/cm^3. The apparent density of the $Mg_2(Sn_{0.97}Ti_{0.03})O_4$ ceramics sintered at 1450–1600 ℃ for 4 h was the highest, reaching 4.54 g/cm^3 at a sintering temperature of 1550 ℃, above which it decreased. The increase in apparent density may be caused by the decrease in the number of pores, and the decrease in apparent density may be caused by the

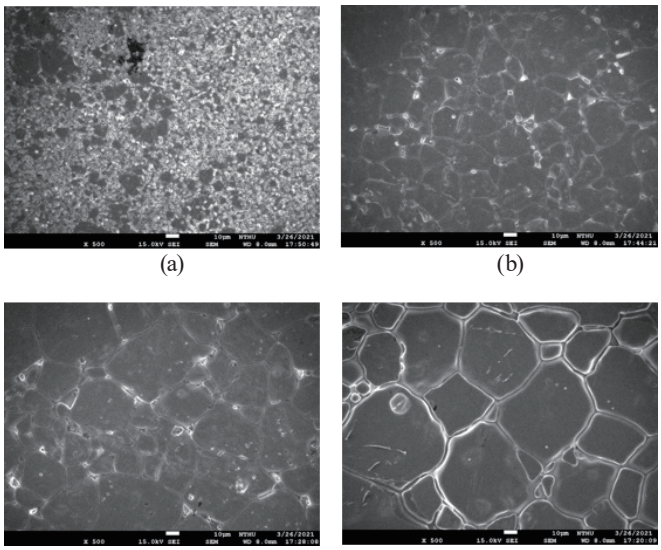

Fig. 2. Microstructures of $Mg_2(Sn_{0.97}Ti_{0.03})O_4$ ceramics following sintering for 4 h at (a) 1450, (b) 1500, (c) 1550, and (d) 1600 °C.

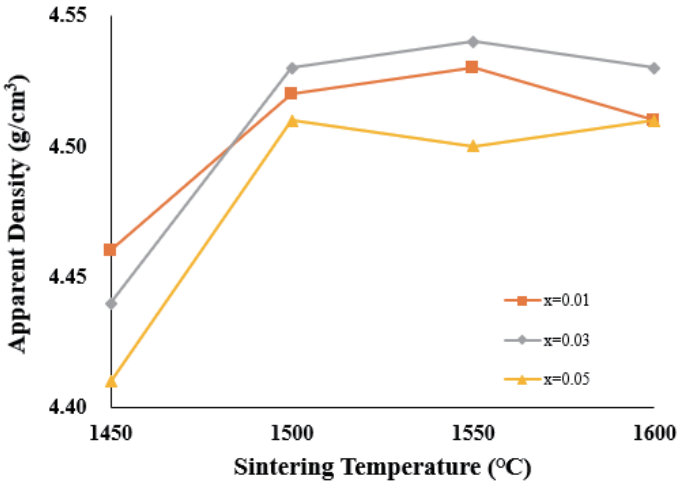

Fig. 3. (Color online) Apparent densities of $Mg_2(Sn_{1-x}Ti_x)O_4$ ceramics with different degrees of Ti^{4+} substitution, following sintering at 1450–1600 °C for 4 h.

porous microstructure, as illustrated in Fig. 2. Although a Ti atom has a smaller mass than a Sn atom, the maximum apparent density increased slightly from 4.53 to 4.54 g/cm^3 as x increased from 0.01 to 0.03.

Figure 4 shows the relative densities of $Mg_2(Sn_{1-x}Ti_x)O_4$ ceramics with different degrees of Ti^{4+} substitution following sintering at 1450–1600 °C for 4 h. The relative density exceeded 93% of the theoretical density (TD) in all cases. A maximum relative density of 95.8% of the TD was obtained for $Mg_2(Sn_{0.97}Ti_{0.03})O_4$ ceramics sintered at 1550 °C for 4 h. The relative density

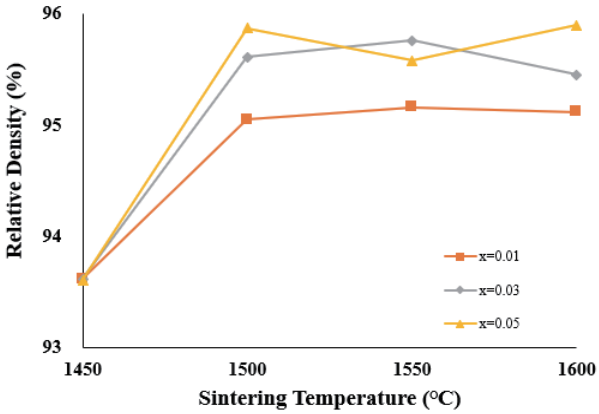

Fig. 4. (Color online) Relative densities of the $Mg_2(Sn_{1-x}Ti_x)O_4$ ceramics with different degrees of Ti^{4+} substitution following sintering at 1450–1600 °C for 4 h.

increased from 94.8% to 95.8% as x increased from 0.01 to 0.03, then decreased to 95.6% as x further increased from 0.03 to 0.05.

Figure 5 shows the dielectric constants of $Mg_2(Sn_{1-x}Ti_x)O_4$ ceramics with different degrees of Ti^{4+} substitution following sintering at 1450–1600 °C for 4 h. The $Mg_2(Sn_{0.97}Ti_{0.03})O_4$ ceramic sintered at 1550 °C for 4 h had a dielectric constant of 8.3. The resonant frequency was approximately 19.0 GHz. A high sintering temperature was not necessary to obtain a high dielectric constant. The decrease in the dielectric constant was associated with low densities of the ceramics. A higher density is associated with lower porosity, and, therefore, a higher dielectric constant. The dielectric constant increased from 7.8 to 8.5 as x increased from 0.01 to 0.05 when $Mg_2(Sn_{1-x}Ti_x)O_4$ ceramics were sintered at 1550 °C for 4 h. These results suggest that the dielectric constant was effectively increased by substituting some of the Sn^{4+} ions with Ti^{4+} ions, which might be explained by ionic polarization. The dielectric constant can be calculated using the Clausius–Mossotti equation, as suggested by Tohdo *et al.*,[11]

$$\varepsilon_r = \frac{3V_m + 8\pi\alpha_D}{3V_m - 4\pi\alpha_D}, \tag{7}$$

where Vm is the molar volume and αD is the sum of polarizations of individual ions. The dielectric constants is dependent on the ionic polarization; the larger the ionic polarization, the higher the dielectric constant. The polarizations of Sn^{4+} and Ti^{4+} ions are 2.83 and 2.93, respectively.[12,13] Moreover, the Ti^{4+} ions with smaller radius occupy Sn^{4+} ions and have a smaller molar volume, resulting in a higher dielectric constant.

Figure 6 shows the quality factor of the $Mg_2(Sn_{1-x}Ti_x)O_4$ ceramics with different degrees of Ti^{4+} substitution following sintering at 1450–1600 °C for 4 h. The $Mg_2(Sn_{0.97}Ti_{0.03})O_4$ ceramics sintered at 1550 °C for 4 h had the highest $Q \times f$ of 75000 GHz. The relationship between $Q \times f$ and the sintering temperature was consistent with that between the relative density and the sintering temperature, because the microwave dielectric loss is affected by many factors and

consists of intrinsic and extrinsic components. Intrinsic loss is associated with lattice vibrational modes. Extrinsic loss is associated with density, porosity, second phases, impurities, oxygen vacancies, grain size, and lattice defects.[14,15] Since the $Q \times f$ of the $Mg_2(Sn_{0.97}Ti_{0.03})O_4$ ceramics was consistent with the variation of relative density, it is suggested to be dominated by the relative density. $Q \times f$ increased from 62800 to 75000 GHz as x increased from 0.01 to 0.03, then decreased to 64,200 GHz as x further increased from 0.03 to 0.05 for the $Mg_2(Sn_{1-x}Ti_x)O_4$ ceramic sintered at 1550 °C for 4h.

Figure 7 shows τ_f of $Mg_2(Sn_{1-x}Ti_x)O_4$ ceramics with different degrees of Ti^{4+} substitution following sintering at 1450–1600 °C for 4 h. Generally, the temperature coefficient of resonant frequency is related to the composition, the amount of additives, and the second phases present in ceramics. Although secondary phases of MgO and SnO_2 were found, the variation in the number of secondary phases with x was not significant, meaning that their influence on the $Mg_2(Sn_{1-x}Ti_x)O_4$ ceramics was small. Since the composition of $Mg_2(Sn_{1-x}Ti_x)O_4$ ceramics with a

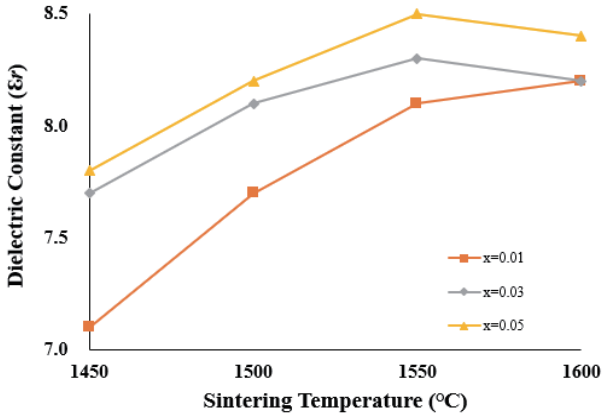

Fig. 5. (Color online) Dielectric constants of $Mg_2(Sn_{1-x}Ti_x)O_4$ ceramics with different degrees of Ti^{4+} substitution following sintering at 1450–1600 °C for 4 h.

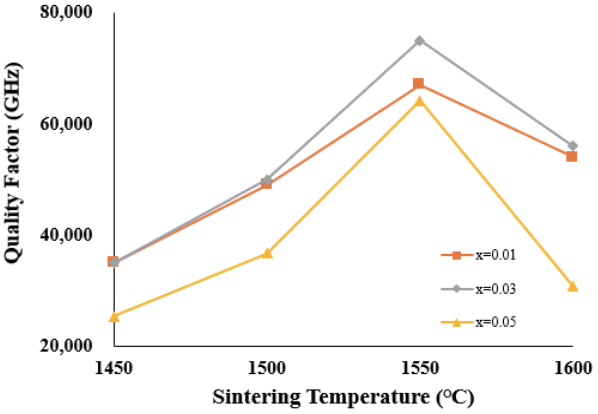

Fig. 6. (Color online) Quality factor of $Mg_2(Sn_{1-x}Ti_x)O_4$ ceramics with different degrees of Ti^{4+} substitution following sintering at 1450–1600 °C for 4 h.

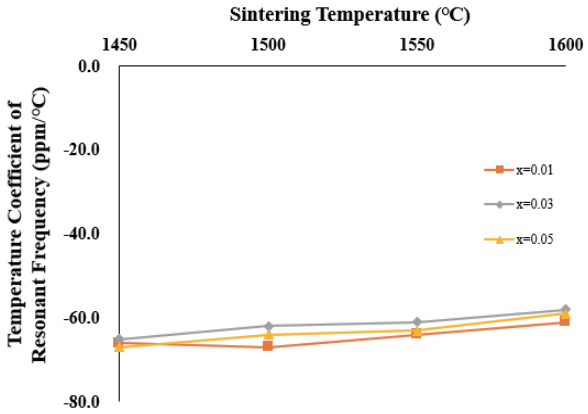

Fig. 7. (Color online) of $Mg_2(Sn_{1-x}Ti_x)O_4$ ceramics with different degrees of Ti^{4+} substitution following sintering at 1450–1600 °C for 4 h.

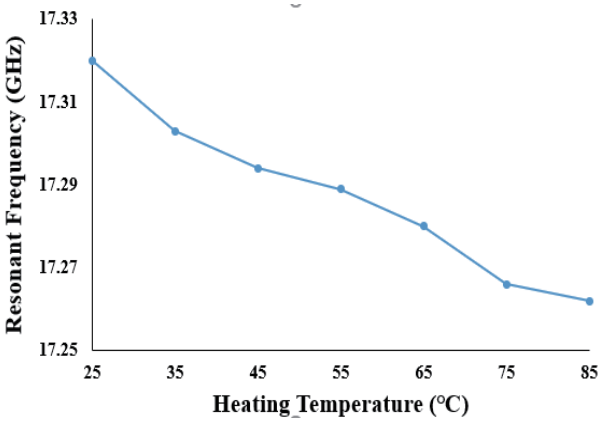

Fig. 8. (Color online) Measured resonant frequency versus temperature.

fixed degree of Ti^{4+} substitution did not vary with sintering temperature, no significant variation in $Mg_2(Sn_{1-x}Ti_x)O_4$ ceramics with sintering temperature was observed over the entire range of sintering temperatures considered herein. A yield of −57 ppm/°C was measured for the $Mg_2(Sn_{0.97}Ti_{0.03})O_4$ ceramic sintered at 1550 °C for 4 h.

Figure 8 shows the measured resonant frequency versus temperature. As the temperature increases from 25 to 85 °C, the resonant frequency decreases from 17.320 to 17.262 GHz. The resonant frequency decreases almost linearly as the operating temperature increases with a linearity of 9.48%. The frequency variation is 58 MHz, which corresponds to a sensitivity of −0.97 MHz/°C, which is higher than that of similar antenna-based temperature sensors.[16–23] The resonant frequency versus temperature exhibited good repeatability in two rounds of measurements. These features mean that the proposed $Mg_2(Sn_{0.97}Ti_{0.03})O_4$ ceramic has high reliability.

4. Conclusions

The effects of the degree of Ti^{4+} substitution and sintering temperature on the microwave dielectric properties of $Mg_2(Sn_{1-x}Ti_x)O_4$ ceramics were studied. The microwave dielectric properties of the $Mg_2(Sn_{1-x}Ti_x)O_4$ ceramics were improved by substituting Sn^{4+} ions with Ti^{4+} ions. The XRD peaks of the $Mg_2(Sn_{0.97}Ti_{0.03})O_4$ ceramic did not vary significantly with the sintering temperature. The $Mg_2(Sn_{0.97}Ti_{0.03})O_4$ ceramic sintered at 1550 °C for 4 h had an apparent density of 4.54 g/cm^3, a dielectric constant of 8.3, a $Q \times f$ of 75000 GHz, and a temperature coefficient of resonant frequency (τ_f) of −57 ppm/°C. The dielectric constant of the $Mg_2(Sn_{1-x}Ti_x)O_4$ ceramics was affected by the relative density and ionic polarization. The $Q \times f$ of the $Mg_2(Sn_{1-x}Ti_x)O_4$ ceramics was affected by the relative density. Fixed degrees of Ti^{4+} substitution have no significant variation in τ_f. In addition, a dielectric resonator temperature sensor was successfully realized with the $Mg_2(Sn_{0.97}Ti_{0.03})O_4$ ceramic. The resonant frequency decreases almost linearly as the operating temperature increases with a linearity of 9.48% and a sensitivity of −0.97 MHz/°C. The structure of the proposed dielectric resonator temperature sensor was simple and easily manufactured. Their robustness, low loss, and high sensitivity make dielectric resonator temperature sensors attractive for further development and application in harsh industrial environments.

Acknowledgments

The authors would like to thank the Ministry of Science and Technology in Taiwan for financially supporting this research under Contract No. MOST 111-2221-E-262-001-.

References

1 C. Mandel, H. Maune, M. Maasch, M. Sazegar, M. Schüßler, and R. Jakoby: Proc. 6th German Microwave Conf. (2011) 1. https://ieeexplore.ieee.org/abstract/document/5760714
2 S. Preradovic and N. Karmakar: IEEE Sensors (2010) 1277. https://doi.org/10.1109/ICSENS.2010.5690591
3 T. Thai, J. Mehdi, H. Aubert, P. Pons, G. DeJean, M. Tentzeris, and R. Plana: IEEE MTT-S Int. Microwave Symp. Digest (2010) 473. https://doi.org/10.1109/MWSYM.2010.5517892
4 A. Traille, M. Tentzeris, S. Bouaziz, P. Pons, and H. Aubert: IEEE Int. Conf. RFID-Technologies and Applications (IEEE, 2012) 398. https://doi.org/10.1109/RFID-TA.2012.6404554
5 Y. C. Chen, Y. N. Wang, and C. H. Hsu: J. Alloys Compd. **509** (2011) 9650. https://doi.org/10.1016/j.jallcom.2011.07.065
6 B. W. Hakki and P. D. Coleman: IEEE Trans. Microwave Theory Tech. **8** (1960) 402. https://doi.org/10.1109/TMTT.1960.1124749
7 Y. Kobayashi and M. Katoh: IEEE Trans. Microwave Theory Tech. **33** (1985) 586. https://doi.org/10.1109/TMTT.1985.1133033
8 G. Pfaff: Thermochim. Acta **237** (1994) 83. https://doi.org/10.1016/0040-6031(94)85186-7
9 E. R. Leite, J. A. Cerri, E. Longo, J. A. Varela, and C. A. Paskocima: J. Eur. Ceram. Soc. **21** (2001) 669. https://doi.org/10.1016/S0955-2219(00)00250-8
10 S. P. Wu and J. H. Luo: J. Alloys Compd. **509** (2011) 8126. https://doi.org/10.1016/j.jallcom.2011.05.079
11 Y. Tohdo, K. Kakimoto, H. Ohsato, H. Yamada, and T. Okawa: J. Eur. Ceram. Soc. **26** (2006) 2039. https://doi.org/10.1016/j.jeurceramsoc.2005.09.098
12 R. D. Shannon: J. Appl. Phys. **73** (1993) 348. https://doi.org/10.1063/1.353856
13 C. Veneis, P. K. Davies, T. Negas, and S. Bell: Mater. Res. Bull. **31** (1996) 431. https://doi.org/10.1016/S0025-5408(96)00028-1
14 B. D. Silverman: Phys Rev. **125** (1962) 1921. https://doi.org/10.1103/PhysRev.125.1921

15 W. S. Kim, T. H. Hong, E. S. Kim, and K. H. Yoon: Jpn. J. Appl. Phys. **37** (1998) 5367. https://iopscience.iop.org/article/10.1143/JJAP.37.5367
16 H. Cheng, S. Ebadi, and X. Gong: IEEE Antennas Wirel. Propag. Lett. **11** (2012) 369. https://doi.org/10.1109/LAWP.2012.2192249
17 X. Ren, S. Ebadi, Y. Chen, L. An, and X. Gong: IEEE Trans. Microwave Theory Tech. **61** (2013) 960. https://doi.org/10.1109/TMTT.2012.2234476
18 Q. Qiao, L. Zhang, F. Yang, Z. Yue, and A. Z. Elsherbeni: IEEE Antennas Wireless Propag. Lett. **12** (2013) 1420. https://doi.org/10.1109/LAWP.2013.2286631
19 H. Cheng, X. Ren, S. Ebadi, Y. Chen, L. An, and X. Gong: IEEE Sens. J. **15** (2015) 1453. https://doi.org/10.1109/JSEN.2014.2363426
20 H. Cheng, S. Ebadi, X. Ren, and X. Gong: Sens. Actuators, A **222** (2015) 204. https://doi.org/10.1016/j.sna.2014.11.010
21 Q. Tan, T. Wei, X. Chen, T. Luo, G. Wu, C. Li, and J. Xiong: Sens. Actuators, A **236** (2015) 299. https://doi.org/10.1016/j.sna.2015.10.052
22 D. Yan, Y. Yang, Y. Hong, T. Liang, Z. Yao, X. Chen, and J. Xiong: Micromachines 8 No. **10** (2017) 301. https://doi.org/10.3390/mi8100301
23 H. Kou, Q. Tan, Y. Wang, G. Zhang, S. Su, and J. Xiong: Sens. Actuators, B **311** (2020) 127907. https://doi.org/10.1016/j.snb.2020.127907

About the Authors

Yih-Chien Chen received his B.S., M.S., and Ph.D. degrees in electrical engineering from National Cheng Kung University, Tainan, Taiwan, in 1994, 1996, and 2000, respectively. He is currently a distinguished professor in the Department of Electrical Engineering, Lunghwa University of Science and Technology, Taoyuan, Taiwan. His research interests are in microwave engineering, microwave ceramics, and sensors. (ee049@mail.lhu.edu.tw)

Chun-Hao Tai received his B.S. degree in electrical engineering from Lunghwa University of Science and Technology, Taoyuan, Taiwan, in 2020. He is currently an M.S. student in the Department of Electrical Engineering, Lunghwa University of Science and Technology, Taoyuan, Taiwan. His research interests are in microwave engineering, microwave ceramics, and sensors. (watermelon87223@gmail.com)

Rei-Shin Chen received his Ph.D. degree in electrical engineering from National Taiwan University, Taipei, Taiwan, in 1996. Since August 2002, he has been with the Department of Electrical Engineering, Lunghwa University of Science and Technology, Taoyuan, Taiwan. His current research interests include integrated optical waveguides, optical fibers, and antenna design. (crs@mail.lhu.edu.tw)